J. Electrical Systems 20-10s (2024): 820-832

[1]Yunpeng Sun

[1]Wei Tang*

Design of Modified Predictive Active Disturbance Rejection Controller for Cross Direction Basis Weight Control Process of Paper Machine

Abstract: - This paper focuses on the demand for accurate cross direction basis weight of paper and proposes a predictive active disturbance rejection controller (ADRC) with good real-time performance and strong robustness, which is effective for processes with large time delays and is applied to the cross direction basis weight of paper. To address the time-varying uncertainties caused by fluctuations in the speed of the paper machine, an ADRC with a feedback filter is utilized to actively estimate and compensate for disturbances. For the significant time delay characteristic of the cross direction basis weight loop, a predictive structure with a weighted average to mitigate the delay is adopted to compensate for the untimeliness caused by the significant delay. This leads to a modified predictive ADRC strategy that can both predict information and compensate for total disturbances, aiming to solve the control challenges in the cross direction basis weight of paper loop due to uncertainties and significant time delay characteristics. The paper first elaborates on the design process of the predictive ADRC, analyzes its stability, and then presents the rules for controller parameter tuning. Finally, it compares the proposed controller with three other controllers with good real-time performance through simulation. The research results indicate that the modified predictive ADRC proposed in this paper has excellent disturbance rejection capability and setpoint tracking performance, with the advantages of simple parameter tuning, good real-time performance, and smooth control process, providing an effective method for process control in the low-carbon papermaking industry.

Keywords: cross direction basis weight of paper; large delay process; active disturbance rejection control; smith predictor; time-varying uncertainty

1. Introduction

Basis weight is one of the most important indicators for assessing paper quality, characterizing the weight of paper per unit area[1]. The widespread use of high-speed printing presses and the trend low basis weight and cardboard have imposed stricter requirements on the uniform distribution of paper fibers[2]. The uniformity of paper primarily reflects in its basis weight; uneven quantitative distribution manifests as uneven thickness across the paper web, often leading to paper jams during high-speed printing operations, severely impacting the printing process and resulting in the wastage of printing resources[3-4]. Basis weight control is divided into longitudinal (Machine Direction, MD) control and cross direction (Cross Direction, CD) control. While longitudinal basis weight has matured, it does not ensure the uniformity of the paper[5-6], hence the development of cross direction basis weight of paper technology. CD basis weight is achieved by controlling the opening degree of a group of dilution water valves (a group of dilution water valves installed at fixed intervals across the width of the paper web) perpendicular to the direction of the paper machine. As shown in Figure 1, the paper quantitative detection location is generally set at the end of the paper machine (where the paper is rolled up), and the actuator (group of dilution water valves) is located on the headbox at the start of the paper machine. The feedback from detection data and

[1] [1]* School of Electrical and Control Engineering, Shaanxi University of Science and Technology,

Xi'an, Shaanxi Province, 710021, China.Email:syp_wangyi@163.com

the adjustment of dilution water valves span the length of the paper machine, thus the paper basis weight process exhibits significant time-delay characteristics, where the system's lag time is directly proportional to the length of the paper machine and the quantitative value, and inversely proportional to the speed of the paper machine. In practice, the speed of the paper machine is not constant, leading to time-varying uncertainties, mainly manifested as variable lag times caused by changing speeds.

In industrial process control, a compensator running in parallel with the controlled plant is often introduced to eliminate the impact of pure time-delay elements on control quality, such as the Smith predictor. Over the years, intelligent control algorithms such as neural network control, fuzzy control[7-8], and various modified algorithms based on the Smith predictor[8-9] have been applied to CD basis weight, achieving good simulation and experimental results. However, considering the difficulty of engineering implementation, disturbance resistance, and real-time requirements of paper CD basis weight control algorithms, few are actually implemented. Active Disturbance Rejection Control (ADRC) has the capability to estimate and actively compensate for internal and external disturbances in real-time, hence it has been widely applied in various uncertain systems over the past decade[10]. Moreover, ADRC has the advantage of requiring less computational effort compared to intelligent control algorithms such as neural network control and fuzzy control, and has been incorporated into the MCU and DSP chips by companies such as Texas Instruments[11].

For the control problem of processes with turbidity processes, which involves complex physical and chemical reactions, is difficult to control for engineers due to its characteristics of large time delays, uncertainties, and numerous disturbances, literature[12] innovatively proposed the integration of Smith prediction and ADRC (Predictive Active Disturbance Rejection Control, PADRC) to forecast process outputs in advance, compensating for the untimeliness of information and thus achieving a predictive ADRC that both actively compensates for total disturbances and predicts information, resulting in effective control. However, due to the high uncertainty of the paper CD basis weight process studied in this paper, the application effect of PADRC is not ideal. This paper designs a modified predictive ADRC (Modified PADRC, M-PADRC) for the paper CD basis weight control process, addressing model mismatches due to changes in paper machine speed, enabling better estimation and compensation for uncertainties under changing model information. The stability of M-PADRC is analyzed from the perspective of transfer functions, and rules for parameter tuning are provided. Simulation studies reveal that M-PADRC achieves good control performance in paper CD basis weight control.

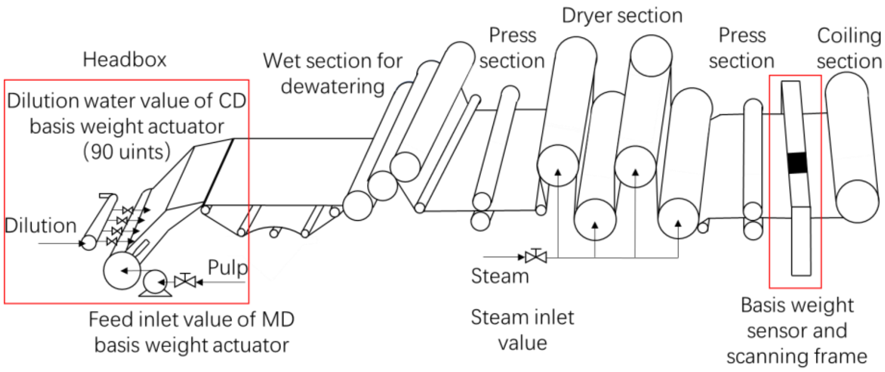

Figure 1. Structure of basis weight control system

2. Basic Principles of Predictive Active Disturbance Rejection Control

2.1. Structure of Linear Active Disturbance Rejection Control

In Active Disturbance Rejection Control (ADRC), "disturbance rejection" essentially means disturbance elimination. The core idea is to estimate and eliminate the total effect of all disturbances on the output of the controlled plant at the input side, making the dynamic quality of the system invariant. This approach does not depend on the dynamic model of the system. It transforms the system by extracting real-time information about internal and external uncertainties, thus maintaining the dynamic quality of the system unchanged and achieving an "invariance" in the dynamic relationship between system input and output. This significantly simplifies the design and parameter tuning of the controller [13]. As illustrated in Figure 2, the Tracking Differentiator (TD) is primarily used for controlling the transition process to avoid the impact of excessive initial errors on the system. However, for processes with large time delays, introducing TD[11] can slow down the system response, so TD is generally not used in such systems. ADRC constructs an Extended State Observer (ESO) based on the input and output feedback signals of the controlled plant to estimate the values of various states and the total disturbance in real-time. The State Error Feedback (SEF) control law uses the estimated value of the total disturbance from ESO to generate control signals to compensate for the disturbance effects on the system.

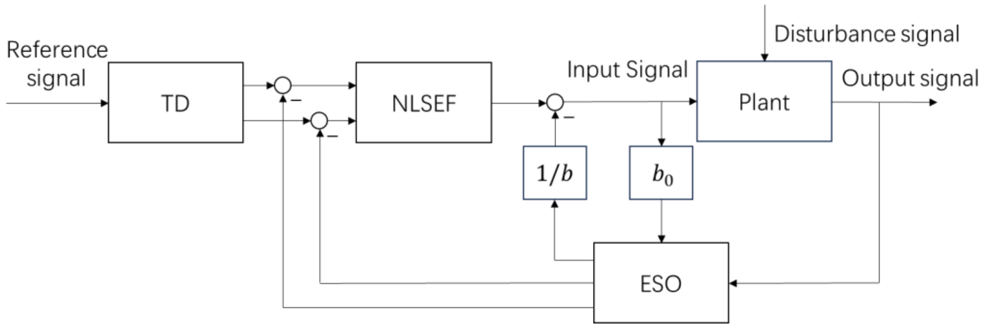

Figure 2. Block diagram of ADRC control

The literature [14] employs linearization processing and pole assignment principles, proposing linear active disturbance rejection control and the corresponding bandwidth tuning method, significantly reducing the number of parameters that need to be adjusted, thus facilitating the engineering implementation of active disturbance rejection control.

The differential equation for a first-order inertial system without time-delay elements is represented as:

$$\dot{y} = bu + f_1(y, w) = -ay + b(u + w) \tag{1}$$

where y represents the controlled output; u represents the control input; a and b are system parameters; $f_1(y, w)$ represents the total original disturbance of the system, including internal disturbances caused by object uncertainties and external disturbances w.

Let b be the estimate of b_0, then $(b - b_0)u$ represents the inaccurate part of the estimate. Letting $f(y, u, w) = -ay + bw + (b - b_0)u$, we can derive equation from the original equation:

$$\dot{y} = f(y, u, w) + b_0 u \tag{2}$$

Let $x_1 = y, x_2 = f$. Assuming the total disturbance f is bounded and differentiable, the extended state equation of the original system is:

$$\begin{cases} \dot{\boldsymbol{X}} = \boldsymbol{AX} + \boldsymbol{B}u + \boldsymbol{E}\dot{f} \\ y = \boldsymbol{CX} \end{cases} \tag{3}$$

where $\boldsymbol{X} = \begin{bmatrix} x_1 \\ x_2 \end{bmatrix}$; $\boldsymbol{A} = \begin{bmatrix} 0 & 1 \\ 0 & 0 \end{bmatrix}$; $\boldsymbol{B} = \begin{bmatrix} b_0 \\ 0 \end{bmatrix}$; $\boldsymbol{C} = \begin{bmatrix} 1 \\ 0 \end{bmatrix}^T$; $\boldsymbol{E} = \begin{bmatrix} 0 \\ 1 \end{bmatrix}$.

Based on equation (3), design the Linear Extended State Observer (LESO):

$$\begin{cases} \dot{\boldsymbol{Z}} = \boldsymbol{AZ} + Bu + \boldsymbol{L}(y - z_1) \\ z_1 = \boldsymbol{CZ} \end{cases} \tag{4}$$

where $\boldsymbol{Z} = [z_1 \quad z_2]^T$ is the observability matrix for $\boldsymbol{X}$, realizing the estimation of the state vector; $\boldsymbol{L} = [\beta_1 \quad \beta_2]^T$ is the gain parameter matrix of the observer.

The control law SEF (State Error Feedback) for ADRC is selected as:

$$u = \frac{[k_1(r - z_1) - z_2]}{b_0} \tag{5}$$

where r represents the reference input; k_1 represents the controller gain.

Assuming the LESO outputs z_1 and z_2 can accurately estimate the system output y and the total disturbance f, respectively, by combining equations (2) and (5), we can derive:

$$\dot{y} \approx k_1(r - y) = u_0 \tag{6}$$

In linear active disturbance rejection control, through the accurate estimation and real-time compensation of the total disturbance by LESO, the controlled plant can be transformed into a simple series of integrators. This not only facilitates the design of the controller but also provides outstanding disturbance suppression capability. Literature [14] has provided the relationship formula between the observer bandwidth and the controller gain, which facilitates the tuning of the controller. The relationship formula is as follows:

$$\boldsymbol{L} = [\beta_1 \quad \beta_2]^T = [2\omega_o \ \ \omega_o^2\ ]^T,\ \ k_1 = \ \omega_c \tag{7}$$

where ω_o represents the bandwidth of the observer; ω_c represents the bandwidth of the controller.

2.2. Basic Principles of Predictive Active Disturbance Rejection Control

The paper CD (Cross Direction) basis weight control process is a typical process with large time delay. The model from the change in dilution water valve opening to the change in paper weight at the paper reel can be represented by a classic First Order Plus Dead Time (FOPDT) model[9].

$$G_p(s) = \frac{K}{Ts + 1} e^{-ls} = \frac{b}{s + a} e^{-ls},\ \ K > 0,\ \ T > 0,\ \ l > 0 \tag{8}$$

where $G_p(s)$ represents the controlled plant; K represents the system gain; T represents the inertia time; l represents the pure delay time constant; $a = 1/T$; $b = K/T$.

The Predictive Active Disturbance Rejection Controller (PADRC) proposed in literature [12], designed for processes with significant turbidity and time delays, can also be represented by a typical FOPDT model.

Under the effect of control input u, the output y of the controlled plant G(s) is represented by a differential equation:

$$\dot{y} = f\ (y, u, w) + bu(t - l) \tag{9}$$

In the equation: $f(y, u, w) = -ay + bw(t - l)$represents the total disturbance, including the internal disturbance $w(t - l)$ caused by parameter a and b perturbations and external disturbances in paper CD basis weight control.

Based on the equation, the state equation and ESO (Extended State Observer) are as follows:

$$\begin{cases} \dot{\boldsymbol{X}}(t - l) = \boldsymbol{AX}(t - l) + \boldsymbol{B}u(t - l) + \boldsymbol{E}\dot{f} \\ y(t - l) = \boldsymbol{CX}(t - l) \end{cases} \tag{10}$$

$$\begin{cases} \dot{\boldsymbol{Z}} = \boldsymbol{AZ}(t) + Bu(t) + L(y(t - l) - z_1(t)) \\ z_1(t) = \boldsymbol{CZ}(t) \end{cases} \tag{11}$$

The discrepancy $y(t - l) - z_1(t)$ in timing $t < l$ of the ESO's error can lead to significant estimation errors or even instability of the ESO. The delay caused by the large delay in information feedback prevents the controller from effectively controlling the process. Therefore, as shown in Figure 3, the Predictive Active Disturbance Rejection Control incorporates a Smith Predictor, using the predicted model output as system feedback information during the initial tracking phase to compensate for the actual output, solving the synchronization issue of the two input signals observed by ESO.

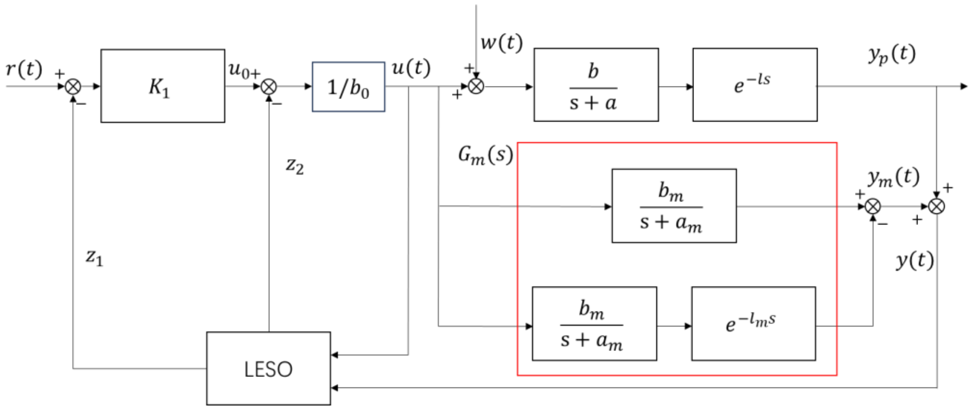

Figure 3. The diagram of predictive active disturbance rejection control

In Figure 3: $r(t)$ represents the reference signal, $u(t)$ represents the control signal output by the controller, $w(t)$ represents the disturbance input signal a, b and l are the parameters of the object model, $G_m(s)$ is the Smith Predictor model with corresponding compensation model parameters a_m , b_m and l_m , $y_m(t)$ represents the output of the predictor model, and is the overlay of the actual output of the object and the output of the predictor model.

When $l \approx l_m$, in the initial phase of tracking, the predicted output is generated by the delay-free part of the predictor model, then gradually transitions to the measured output, and adjusts through the controller for errors caused by model mismatch and disturbances until it reaches a steady state.

3. Design and Analysis of Modified Predictive Active Disturbance Rejection Control

3.1. Design of Modified Predictive Active Disturbance Rejection Controller

Although PADRC has the capability to estimate the total disturbance based on the feedback of the actual output of the object and the control signal output by the controller, the Smith Predictor relies too heavily on the system model of the controlled plant. In the paper CD basis weight process, changes in the paper machine speed and the resulting changes in the system model can lead to poor control performance or even instability of the control system. This project designs a Modified Predictive Active Disturbance Rejection Controller, as shown in Figure 4, to optimize control performance in the paper CD basis weight process.

The Pade approximation can rationalize the pure delay terms through rational polynomial approximation. A first-order Pade approximation can be described as:

$$e^{-ls} \approx \frac{2 - ls}{2 + ls} \tag{12}$$

After replacing l with $l/p_m (p_m \geq 1)$ and using a first-order Pade approximation, we can obtain P_m:

$$e^{-\frac{l}{p_m}s} \approx \frac{2p_m - ls}{2p_m + ls} = P_m \tag{13}$$

Based on predictive active disturbance rejection control, this paper designs a weighted average structure based on Pade approximation, allowing system feedback information in the initial phase of tracking to smoothly transition to measured output with ADRC, improving system stability and dynamic performance. Moreover, by introducing a new difference signal between the actual model and the predictor model through a first-order filter on the loop's periphery, the effect of model mismatch is mitigated, enhancing system robustness.

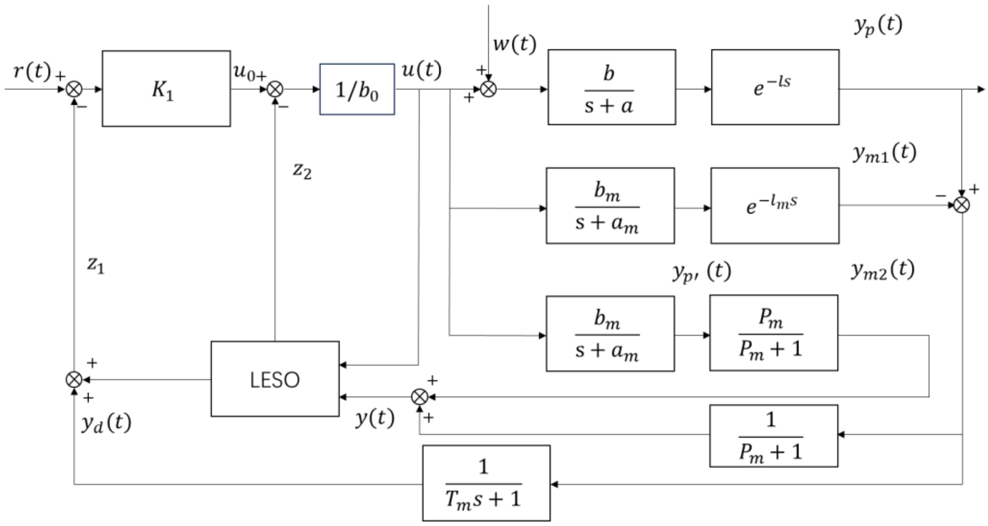

Figure 4. The diagram of modified PADRC

In Figure 3, a_m , b_m and l_m are the compensation model parameters, $y_p(t)$ is the output of the original controlled plant, $y_{m1}(t)$ is the output of the predictor model, $y_{p'}(s)$ is the model output before weighting, $y_{m2}(t)$ is the model output after weighting, $y_d(t)$ is the output of a first-order low-pass filter processing the difference signal $y_p(s) - y_{m1}(t)$ between the actual model and the predictor model, $y(t)$ is the feedback signal of LESO, $P_m = (2p_m - 2)/(l_m s + 2)$, p_m are approximation parameters ($p_m \geq 1$), and T_m is the filter coefficient.

When the compensation model matches the actual model, to address the issue of asynchronous error $y(t-l) - z_1(t)$ in ESO at $t < l$, drawing from the Smith Predictor, using the output of the predictor model as system feedback information to compensate for the actual output can solve the issue of ESO tracking asynchrony and the problem of missing information at the beginning of tracking in systems with significant delays.

When there is a large discrepancy between the compensation model and the actual model, $y(t) = [1/(P_m + 1)]y_p(t) + [(P_m/(P_m+1)]y_{p'}(t)$.When $P_m \to 0$, $y(t) \to y_p(t)$; when $P_m \to \infty$, $y(t) \to y_{p'}(t)$; when $P_m \in (0, \infty)$, the feedback signal $y(t)$ is a weighted average of the actual process with delay and the nominal model without delay, with the delay time effectively being some value between $(0, l)$. Adjusting P_m can improve the delay time.

The signal after weighted averaging fed back to LESO:

$$y(t) = \frac{1}{P_m + 1} y_p(t) + \frac{P_m}{P_m + 1} y_{p'}(t) = \left(\frac{b}{s+a} e^{-ls} + \frac{b_m}{s+a_m} \frac{2p_m - 2}{l_m s + 2}\right)\left(\frac{l_m s + 2}{l_m s + 2p_m}\right) \quad (14)$$

Given the Pade approximation as shown in the equations:

$$y(t) \approx \frac{b}{s+a} \frac{2p_m - ls}{2p_m + ls} \approx \frac{b}{s+a} e^{-\frac{l}{p_m}s} \quad (15)$$

From equation (15), it is known that when P_m is sufficiently large and when a_m and b_m are not significantly different from the system parameters a and b, $y(t) \approx b/(a+b)$. The Modified Predictive Active Disturbance Rejection Controller can reduce the lag time of the controlled plant, and the internal disturbances introduced by the two Pade approximations can be compensated by LESO. Moreover, by filtering the error signal $y_d(t)$ through a first-order filter and then feeding it back into the forward path, the impact of model mismatch can be mitigated, enhancing the system's robustness.

3.2 Stability Analysis

Under zero initial conditions, based on Figure 3 and equations (4), (7), the transfer functions for the ESO estimated output z_1 and z_2 are respectively:

$$z_1 = \frac{2\omega_o s + {\omega_o}^2}{(s+\omega_o)^2} y_{m2}(s) + \frac{b_0 s}{(s+\omega_o)^2} u(s) + \left(\frac{1}{P_m + 1}\right)\left(\frac{2\omega_o s + {\omega_o}^2}{(s+\omega_o)^2}\right)\left(y_p(s) - y_{m1}(t)\right) \quad (16)$$

$$z_2 = \left(\frac{\omega_o}{s+\omega_o}\right)^2 s y_{m2}(s) + \left(\frac{\omega_o}{s+\omega_o}\right)^2 b_0 u(s) + \left(\frac{1}{T_m s + 1}\right)\left(\frac{\omega_o}{s+\omega_o}\right)^2 s\left(y_p(s) - y_{m1}(t)\right) \quad (17)$$

Substituting equations (16), (17) into equation (5), the transfer function expression (18) can be obtained:

$$u(s) = \frac{(s^2 + 2\omega_o s + {\omega_o}^2)}{\{b_0[s^2 + (k_1 + 2\omega_o)s](P_m + 1) + [(2k_1\omega_o + {\omega_o}^2)s + k_1{\omega_o}^2]P_m G_{m1}\}} \cdot$$

$$\left[k_1 r(s) - \frac{(2k_1\omega_o + {\omega_o}^2)s + k_1{\omega_o}^2}{(s^2 + 2\omega_o s + {\omega_o}^2)(P_m + 1)} y_p(s) - \frac{1}{T_m s + 1}\frac{(2k_1\omega_o + {\omega_o}^2)s + k_1{\omega_o}^2}{(s^2 + 2\omega_o s + {\omega_o}^2)} y_d(s)\right] \quad (18)$$

where $G_{m1} = b_m/(s + a_m)$.

Based on the equation (15), the simplified loop structure of the M-ADRC Predictive Active Disturbance Rejection Control is depicted as shown in Figure 5:

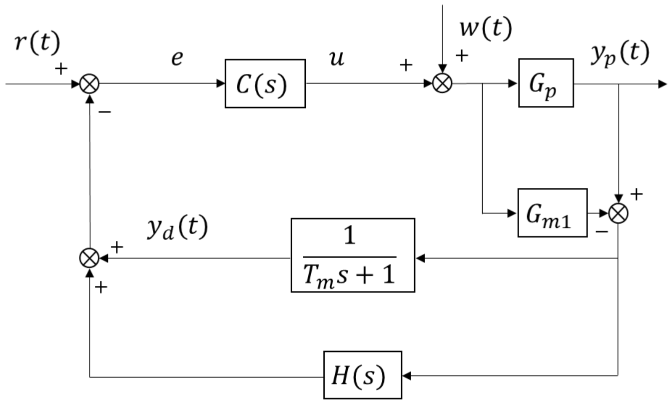

Figure 5. The simplified loop diagram of M-PADRC

In Figure 5:

$$C(s) = \frac{u(s)}{e(s)} = \frac{(s^2 + 2\omega_o s + {\omega_o}^2)}{\{b_0[s^2 + (k_1 + 2\omega_o)s](P_m + 1) + [(2k_1\omega_o + {\omega_o}^2)s + k_1{\omega_o}^2]P_m G_{m'}\}} =$$

$$\frac{B_4 s^4 + B_3 s^3 + B_2 s^2 + B_1 s^1 + B_0}{A_4 s^4 + A_3 s^3 + A_2 s^2 + A_1 s^1 + A_0} \quad (19)$$

$$H(s) = \frac{(2k_1\omega_o + {\omega_o}^2)s + k_1{\omega_o}^2}{(s^2 + 2\omega_o s + {\omega_o}^2)(P_m + 1)} = \frac{C_3 s^3 + C_2 s^2 + C_1 s^1 + C_0}{B_4 s^4 + B_3 s^3 + B_2 s^2 + B_1 s^1 + B_0} \quad (20)$$

The open-loop transfer function $G_O(s)$ is given by:

$$G_O(s) = C(s)G_p(s)H(s) = \frac{C_3 s^3 + C_2 s^2 + C_1 s^1 + C_0}{A_4 s^4 + A_3 s^3 + A_2 s^2 + A_1 s^1 + A_0} G_p(s) \quad (21)$$

where $A_4 = b_0 l_m$; $A_3 = b_0 l_m(2\omega_o + k_1) + b_0(2p_m + a_m l_m)$;

$A_2 = b_0 l_m(2\omega_o + k_1)(2p_m + a_m l_m) + 2b_0 p_m a_m$;

$A_1 = 2b_0 p_m a_m(2\omega_o + k_1) + b_m(2p_m - 2)(2k_1\omega_o + {\omega_o}^2)$;

$A_0 = 2b_m(2p_m - 2)k_1{\omega_o}^2$; $C_3 = l_m(2k_1\omega_o + {\omega_o}^2)$;

$$C_2 = l_m k_1 \omega_o^2 + (2k_1\omega_o + \omega_o^2)(2 + a_m l_m);$$

$C_1 = k_1\omega_o^2(2 + a_m l_m) + 2a_m(2k_1\omega_o + \omega_o^2);\ C_0 = 2a_m k_1 \omega_o^2.$

(1) When $l_m = 1$,

$$G_O(s) = \frac{(2k_1\omega_o + \omega_o^2) + k_1\omega_o^2}{b_0[s^2 + (2\omega_o + k_1)s]} G_p(s) \tag{22}$$

The open-loop transfer function (21) is denoted by a conventional linear active disturbance rejection control open-loop gain, with open-loop poles at $s_1 = 0$ and $s_2 = -(2\omega_o + k_1)$.

(2) When $l_m \neq 1$,

$$G_O(s) = \frac{[(2\omega_o k_1 + \omega_o^2)s + k_1\omega_o^2] \cdot G_p(s)}{p_m\left[b_0 s^2 + \left(b_0(2\omega_o + k_1) + \frac{b_m}{a_m}(2\omega_o k_1 + \omega_o^2)\right)s + \frac{b_m}{a_m}k_1\omega_o^2\right]} \tag{23}$$

When k_1 and ω_o remain constant, the open-loop poles of equation (23) move to the left in the s-plane compared to equation (22), thus the Modified Predictive Active Disturbance Rejection Controller enhances the system stability.

3.3 Parameter Tuning

Based on the simplification of the equation (7), the Modified Predictive Active Disturbance Rejection Controller requires tuning of five parameters: b_0 , ω_o , ω_c , p_m , and T_m. Among these, a larger p_m implies a greater degree of conversion of significant delays into smaller p_m, and a lesser degree of mismatch between the two input signals into ESO during model mismatch. Through extensive simulations, it is generally found that setting $p_m \geq l_m/T$ to a certain value yields good results.

Practical simulation experiments have shown that when there is a model mismatch, if T_m is too small, it can cause the system to overshoot significantly and oscillate; if T_m is too large, the response speed is too slow. When $T_m \geq l_m$, the filter can be very effective. Therefore, $T_m \geq l_m$ is used as a reference initial value for the filter coefficient, with fine adjustments made according to the actual situation to balance the system's speed and stability. For the control requirements of the paper CD basis weight system, a larger b_0 is initially selected to ensure system stability, then set $p_m = 2l_m/T$ and $T_m = l_m$. Afterwards, ω_c and ω_o are adjusted to stabilize the system response, followed by fine-tuning of control parameters as required by the controlled system. To ensure the paper CD basis weight quantitative control system has a large delay margin and minimal overshoot, the parameters for M-PADRC are tuned to:

$$\mathrm{b_0} = (2\sim5)\cdot \mathrm{b},\ \ \omega_\mathrm{o} = (2\sim5)\cdot\omega_\mathrm{c} \tag{24}$$

4. Simulation Experiments Results and Analysis

For a pilot paper mill with a speed of 450 $450\,m/min$ and a basis weight of $66\,g/m^2$, where the basis weight fluctuation is within $2g/m^2$, the parameters of the FOPDT model in equation (8) were obtained through experimental modeling: system gain $K = 1.14$, inertia time $T = 2.43$, and pure delay time $l = 8$. The quantitative loop mathematical model is approximated by equation (24).

$$G(s) = \frac{Y(s)}{R(s)} = \frac{1.14}{2.43s + 1}e^{-8s} \tag{25}$$

where $Y(s)$ is the basis weight; $R(s)$ is the pulp valve opening degree.

From equation (24), it is known that the system has large time-delay (($l/T = 3.29$) characteristics, and due to the variability in paper machine speed, the operating time is uncertain, leading to significant time-varying uncertainty.

The system is subject to numerous internal and external disturbances; hence a Modified Predictive Active Disturbance Rejection Controller is used to control this process.

4.1. Simulation Results under Nominal Model

In the simulation, a negative unit step signal of 50% amplitude is applied at $t = 80s$, and this algorithm is compared with PADRC, the self-tuning Smith Predictor (FuzzyPID-FSmith) introduced in literature [8], and linear ADRC. PADRC and ADRC are tuned using the methods provided in literature [12]; M-ADRC uses the same $b_0, \omega_o, \omega_c, p_m = 6.58, T_m = 8$ as PADRC; initial parameters of FuzzyPID-FSmith are obtained via the Dahllin method.

The controlled output and control quantity output of the object under the parameters in Table 1 are shown in Figure 6. Figure 6 demonstrates that when the predictive model perfectly matches the actual model, M-PADRC achieves faster and more accurate tracking performance and quicker disturbance recovery capability compared to other controllers, and the control signal is more stable during the tracking phase.

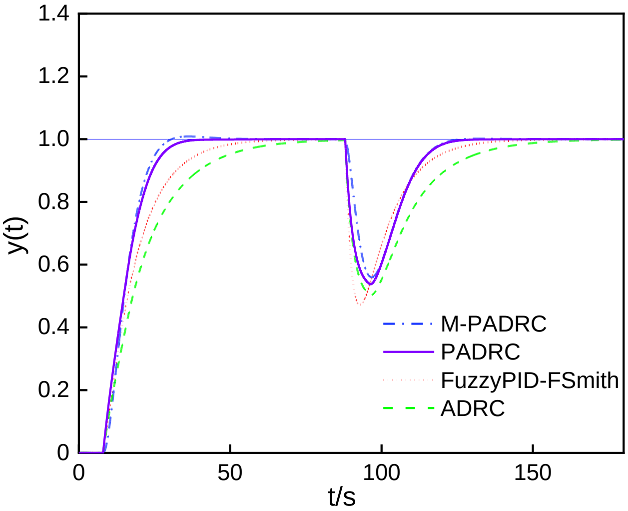

Figure 6. the System response curve in nominal model

Under the nominal model, the parameter tuning results for the four algorithms are shown in Table 1, where the table shows the self-tuning initial values for FuzzyPID-FSmith. The robust tests under parameter perturbation in section 4.2 and delay change in section 4.3 both use this set of parameters.

Table 1. Parameters tuning of four controllers

Controller Type	$b_0(K_p)$	$\omega_c(K_i)$	$\omega_o(K_d)$	P_m	T_m
M-ADRC	2×1.14/2.43	1.96	$3.2 \times \omega_c$	6.58	8
PADRC	2×1.14/2.43	1.96	$3.2 \times \omega_c$	/	/
FuzzyPID-FSmith	2.08	0.55	0	/	/
ADRC	2.9×1.14/2.43	2.05	$2.5 \times \omega_c$	/	/

4.2. Simulation Results for Model Mismatch of the controlled plant

In this robustness test simulation, a larger range of model parameter perturbations was selected: a 20% increase in gain, a 30% increase in inertia time, and a 10% decrease in delay time, resulting in the system response and controller output as shown in Figure 7.

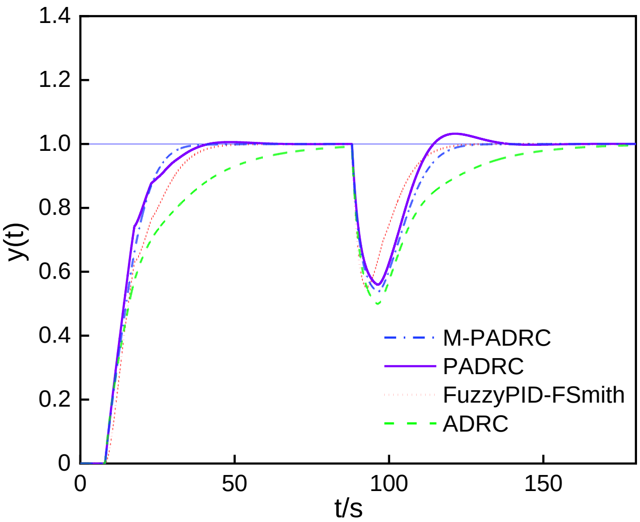

Figure 7. the System response curve in model mismatch

Figure 6 shows that when there are significant changes in model gain and inertia time, and minor changes in delay time, M-PADRC can quickly, smoothly, and accurately track the setpoint and suppress disturbances during both the tracking phase and disturbance recovery phase. Although PADRC responds slightly faster than M-PADRC during the tracking phase, its control signal fluctuates, which is detrimental to the lifespan of the actuators and energy saving. Additionally, its disturbance recovery time is longer than that of PADRC. Both FuzzyPID-FSmith and ADRC algorithms exhibit lengthy adjustment times.

4.3. Simulation Results for Changes in the Lag Time of the controlled plant

When the paper machine speed increases, the delay time will decrease slightly, and when the paper machine speed decreases, the delay time will increase slightly. Figure 8 shows the system dynamic response curve when the delay increases by 20%.

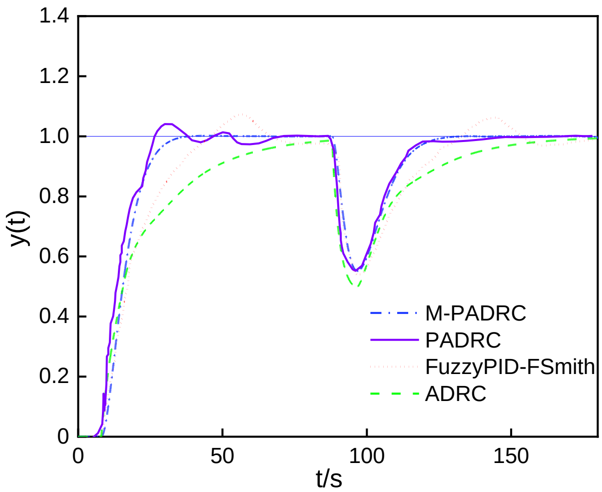

Figure 8. the System response curve when time delay increased 20%

Figure 7 indicates that when there is a significant increase in delay, the system under the effect of M-PADRC achieves better control performance than the other controllers. In the tracking setpoint phase, both PADRC and M-PADRC track quickly, but under M-PADRC control, the controlled quantity has a smaller overshoot and quickly enters a steady state without steady-state error, and the control signal is relatively smoother, which is beneficial for the actuators and energy saving. Under the effect of PADRC and FuzzyPID-FSmith, the controlled quantity experiences overshoot and continuous jitter, and the control signal oscillates significantly, which is very detrimental to the actuators and energy-consuming, not meeting the needs of the low-carbon papermaking industry. ADRC is the slowest and performs worse than FuzzyPID-FSmith. During the disturbance phase, the PADRC algorithm experiences a slight overshoot in the initial short period but quickly returns to the pre-disturbance steady state. The FuzzyPID-FSmith algorithm struggles to track the setpoint for a relatively long initial period, whereas M-PADRC, compared to both FuzzyPID-FSmith and PADRC, has a relatively smoother control signal.

5. Conclusions

This paper designs a Modified Predictive Active Disturbance Rejection Controller based on Pade approximation and weighted average to mitigate delay structure for controlling the paper CD basis weight process and compares this algorithm with conventional ADRC, FuzzyPID-FSmith, and predictive active disturbance rejection control through simulation.

Simulation results show:

(1) Under the nominal model, M-PADRC adopted in this paper achieves good control performance in terms of steady-state error, overshoot, and disturbance resistance and meets the requirements for the speed of the paper CD basis weight process.

(2) Under model parameter perturbation, with significant perturbations in model gain and inertia time, and minor changes in delay time, M-PADRC obtains better tracking ability and faster disturbance recovery ability than FuzzyPID-FSmith and PADRC. Compared to the PADRC controller, although there is no advantage in system output during the tracking phase, the controller output is smoother, reducing wear on the actuators for dilution water valves in the paper CD basis weight process and speeding up the disturbance recovery phase.

(3) When the delay time changes by 20%, its control effect during the tracking setpoint phase is significantly better than the other three algorithms, to some extent overcoming model disturbances caused by changes in vehicle speed and time-varying uncertainty.

Overall, the PADRC controller provides smooth control, strong tracking ability, can reduce the occurrence of paper jams, minimize resource wastage, beneficial for reducing carbon emissions in the papermaking industry; has good real-time performance, fast computational speed, and is easier to implement in engineering compared to advanced intelligent algorithms; and can overcome significant delays and time-varying uncertainties in cross direction basis weight of paper to some extent.

Supplementary Materials: The following supporting information can be downloaded at: www.mdpi.com/xxx/s1, Figure S1: title; Table S1: title; Video S1: title.

Author Contributions: Conceptualization, Y.S.; software, Y.S.; validation, Y.S.; formal analysis, Y.S.; data curation, Y.S.; writing—original draft, W.T.; writing—review and editing, Y.S. and W.T. All authors have read and agreed to the published version of the manuscript.

Funding: This research was funded by National Natural Science Foundation of China, grant number 62073206.

Institutional Review Board Statement: Not applicable

Informed Consent Statement: Not applicable.

Data Availability Statement: We encourage all authors of articles published in MDPI journals to share their research data. In this section, please provide details regarding where data supporting reported results can be found, including links to publicly archived datasets analyzed or generated during the study. Where no new data were created, or where data is unavailable due to privacy or ethical restrictions, a statement is still required. Suggested Data Availability Statements are available in section "MDPI Research Data Policies" at https://www.mdpi.com/ethics.

Conflicts of Interest: The authors declare no conflict of interest.

References

[1] SHANG M, MA W M. Application of Fuzzy Self-tuning Control Algorithm in Cross Direction Basis Weight Control[J]. China Pulp & Paper, 2018,37(08):55-60.

[2] SHAN W J, TANG W. Effect of Dilution Water on Pulp Consistency in Cross-directional Basis Weight Control[J]. Palpu Chongi Gisul/Journal of Korea Technical Association of the Pulp and Paper Industry,2019,51(2):3-15.

[3] XIONG Z X, HU M Y, CHEN Z X, et al. Comprehensive Quality Evaluation of Paper and Cardboard Based on Projection Pursuit Model[J]. Packaging Engineering, 2010,31(05):45-48.

[4] LI Z J, LIU L, CHEN Y C. Study of Printability Comprehensive Assessment System of Offset Paper[J]. Packaging Engineering,2009,30(01):81-83.

[5] LIU W B, WANG X, TANG W, et al. Study and Application of Cross Direction Basis Weight Control System Based on Dilution Water Adjustment[J]. China Pulp ＆ Paper,2014,33(8):1-6.

[6] LIU W B, TANG W, WANG X, et al. Application of Wavelet Denoise Method in Paper Cross Direction Basis Weight Data Treatment[J]. Transactions of China Pulp and Paper,2015,30(2):53-57.

[7] SHAN W J, TANG W, WANG M X, Application of Fractional Order PID Controller Based on Neural Network to Pulp Consistency Control System[J]. Transactions of China Pulp and Paper,2016,31(04):44-48.

[8] TANG W, ZHANG X, LIU W B, et al. Design of Self-tuning Smith Predictor with Feedback Filter and Application in Cross Direction Basis Weight Control of Paper Machine[J]. China Pulp ＆ Paper, 2023,42(02):110-118.

[9] SHAN W J, TANG W, WANG M X, et al. Two-degree-of-freedom Smith Predictor Based on Fractional Order PID Controller in Paper Basis Weight[J]. Packaging Engineering, 2017,38(11):143-147.

[10] WANG L J, LI Q, TONG C N, et al. Overview of active disturbance rejection control for systems with time-delay[J]. Control Theory & Applications,2013,30(12):1521- 1533.

[11] XUE W C, HUANG Y. On performance analysis of ADRC for nonlinear uncertain systems with unknown dynamics and discontinuous disturbance[C] //Proceeding of the 32nd Chinese Control Conference. Xi’an, China: IEEE, 2013:1102-1107.

[12] TANG D C, GAO Z Q, ZHANG X H, Design of predictive active disturbance rejection controller for turbidity[J]. Control Theory & Applications, 2017, 34(01):101-108.

[13] GAO Z Q. On the Problem of Information in Engineering Cybernetics[J]. Journal of Systems Science and Mathematical Sciences, 2016,36(07):908-923.

[14] GAO Z Q. Scaling and bandwidth-parameterization based controller tuning[C]//Proceedings of the American Control Conference. Denver: IEEE, 2003: 4989-4996

FUNDING

This work was supported by grants from the National Natural Science Foundation (62073206)

ABOUT THE AUTHOR

Yunpeng Sun was born in Xuchang,Henan,P.R. China, in 1998.He received the B.S. degree in Electrical Engineering and Intelligent Control from Logistics Engineering college,Shanghai Maritime University, Shanghai, China, in 2020, where he is currently pursuing the M.S. degree. His research interests include the paper basis weight control.

E-mail: syp_wangyi@163.com

Wei Tang was born in Xinyang,Henan,P.R. China, in 1971.

Education history:Bachelor's degree in Engineering from the Department of Automation, Shaanxi University of Science and Technology;Master's degree in Engineering from the Department of Automation, Shaanxi University of Science and Technology;Studied in the Department of Electrical and Information Engineering at Nagoya Institute of Technology, Japan;Postdoctoral/visiting scholar research at Nagoya Institute of Technology, Japan (sponsored by the national program).

Career history:have been teaching at Shaanxi University of Science and Technology since July 1997;was promoted lecturer in 2000, associate professor in 2003, professor in 2007;was promoted Level-3 professor in 2013;

Research interests:papermaking automation;automation of the entire process of pulp and paper making;advanced control of industrial processes;control and application of processes with large time delays.

E-mail: tangwei@sust.edu.cn